

# Application of different MPPT techniques in performances evaluation of a PV pumping system

Ahmed Mohammedi, Nabil Mezzai, Zahra Mokrani, Djamila Rekioua

Department of Electrical Engineering, Laboratory LTII, University of Bejaia,

A/MIRA university, Bejaia 06000, Algeria

mohammedi\_ahmed06@yahoo.fr

**Abstract**— The maximum power point tracking (MPPT) is the automatic control algorithm to adjust the power interfaces and achieve the greatest possible power harvest, during moment to moment variations of light level, shading, temperature, and photovoltaic (PV) module characteristics. It has become an essential component to evaluate the design performance of PV power systems. Direct Torque Control (D.T.C) method is based on instantaneous space vector theory. By optimal selection of the space voltage vectors in each sampling period, D.T.C archives effective control of the stator flux and torque. This paper describes a D.T.C of an induction motor (I.M) associated to a photovoltaic water pumping system. In this work a Comparison of two algorithms developed in order to maximize the output power of the PV pumping system for the same given set of conditions. The MPPT methods proposed in this study are two different algorithms: Perturb & Observe (P&O) and sliding mode control (SMC). Results obtained by simulation are presented and discussed.

**Keywords**— MPPT, Pumping system, D.T.C, Induction motor, Sliding Mode Control.

## I. INTRODUCTION

The growing energy demand coupled with the possibility of reduced supply of conventional fuels, evidenced by petroleum crisis, along with growing concerns about environmental conservation, has driven research and development of alternative energy sources that are cleaner, are renewable, and produce little environmental impact[1].

The PV pumping has become one of the most promising fields in PV applications. To achieve the operation's most reliable and most economical; more attention is paid to their design and their optimal use [2]. The demand of PV generation systems seems to be increased for both standalone and grid-connected modes of PV systems. Therefore, an efficient MPPT technique is necessary that is expected to track the MPP at all environmental conditions and then force the PV system to operate at that MPP point [3].

Since the earliest MPPT method published in 1960s, we can count over than fifteen MPPT methods. They can be classified following to MPP process seeking into indirect and direct method. The indirect methods, such short-circuit and open-circuit methods, need a prior evaluation of the PV panel, or are based on mathematical relationships or database not valid for all operating meteorological conditions. So, they cannot obtain exactly the maximum power of PV panel at any irradiance and cell temperature. On the other side, the direct methods operate at any meteorological condition. The most

used methods among them are: Perturb and Observe (P&O), Incremental Conductance (INC), and Fuzzy Logic (FL) based MPPT [4]. A sliding mode control (SMC) is applied to track maximum power of PV system. The advantages of this control are various and important: high precision, good stability, simplicity, invariance, robustness etc... This allows it to be particularly suitable for systems with imprecise model [5].

The basic concept of direct torque control (DTC) of induction-motor drives is to control both stator flux-linkage and electromagnetic torque of the machine simultaneously by using a switching vector look-up table [6], [7].

In this paper we present a proposed DTC-IM structure of an isolated photovoltaic water pumping system. In order to optimize the photovoltaic energy generation, a comparison of two MPPT is analysed. The P&O and SMC were applied to the studied system. The studied system is modelled and simulated in the MATLAB Simulink environment and obtained results are presented.

## II. PROPOSED SYSTEM

The structure illustrated by Fig.1; with two static converters and convention Direct Torque Control is used in this work. The DC-DC converter which is included in this configuration is intended to implement the MPPT control algorithm and to keep the DC bus voltage to the value of the optimal voltage of PV module. The voltage inverter is used to perform DC-AC conversion and to control the mechanical motor speed.

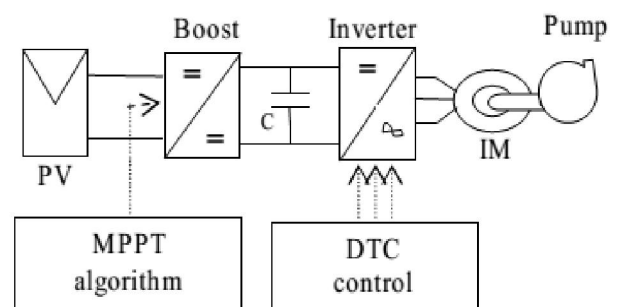


Fig. 1. Proposed system

## III. SYSTEM MODELLING

### A. PV panel modelling

The PV module is a nonlinear device and can be represented by its I-V characteristic. Assuming identical PV cells, the I-V characteristic of the PV module is obtained depending on the

global irradiance and the junction temperature. There are several mathematical models which describe the I-V characteristic [8]. The equivalent circuit (Fig.2) consists of a single diode for the cell polarization phenomena and two resistors (series and shunt) for the losses [26].

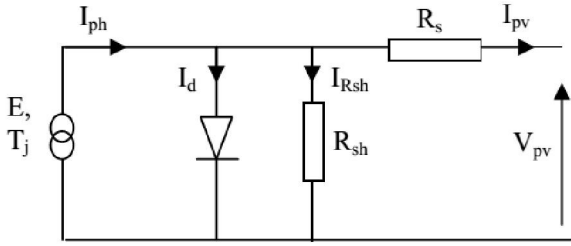


Fig. 2. The equivalent circuit of PV cell

Based on this circuit model, behaviour of the PV module may be described by the following equations [2].

$$I_{pv} = I_{ph} - I_d - I_{Rsh} \quad (1)$$

$$I_{pv} = I_{ph} - I_0 \left[ \exp \left[ \frac{q(V_{pv} + I_{pv} \cdot R_s)}{AnKT} \right] - 1 \right] - \frac{V_{pv}}{R_{sh}} \quad (2)$$

The photocurrent,  $I_{ph}$ , is directly dependent upon both insolation and panel temperature, and may be written in the following form:

$$I_{ph} = P_1 \cdot E_s \cdot [1 + P_2 \cdot (E_s - E_{sref}) + P_3 \cdot (T_j - T_{jref})] \quad (3)$$

Where:  $E$  insolation in the panel plane ( $W/m^2$ );  $E_{sref}$  corresponds to the reference insolation of  $1000 W/m^2$  and  $T_{jref}$  to the reference panel temperature of  $25^\circ C$ .  $P_1$ ,  $P_2$  and  $P_3$  are constant parameters.

The polarization current  $I_d$  of junction PN, is given by the expression:

$$I_d = I_0 \left[ \exp \left[ \frac{q(V_{pv} + I_{pv} \cdot R_s)}{AnKT} \right] - 1 \right] \quad (4)$$

Where:  $I_0$  Cell reverse saturation current (A),  $n$  Ideal constant of diode (1-2),  $q$  the elementary charge (C),  $k$  Boltzman's constant (J/k),  $A$  ideality factor of the junction, and  $R_{se}$ ,  $R_{sh}$  ( $\Omega$ ) resistors (series and shunt). Table 1 shows the parameter of the PV panel Siemens SM 110-24 used in this study.

TABLE I  
PARAMETER OF THE PV PANEL SIEMENS SM110-24

Parameter	Value
$P_{mpp}$	110W
$I_{mpp}$	3.15A
$V_{mpp}$	35V
$I_{sc}$	3.45A
$V_{oc}$	43.5V

Figure 3 shows the current/voltage and power/voltage characteristics represented in standard test conditions:

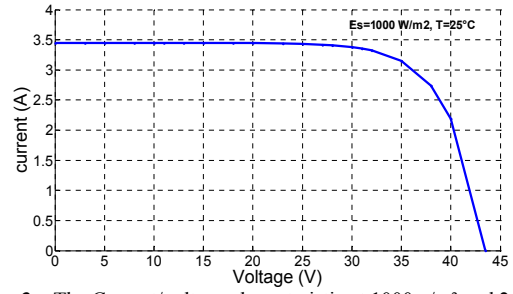


Fig. 3.a. The Current/voltage characteristic at 1000w/m² and 25°C

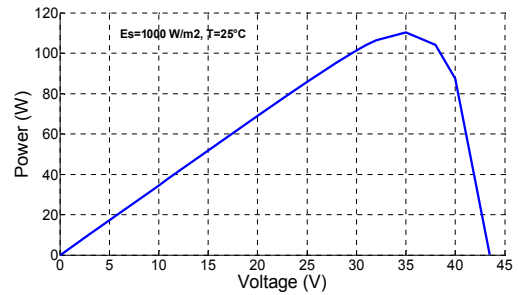


Fig. 3.b. The power/voltage characteristic at 1000w/m² and 25°C

### B. DC/DC converter modeling

The DC-DC converter is a buck, a boost, or a buck-boost chopper in general. It is inserted between the PV generator and its load in order to adjust the dynamic equivalent impedance of the PWM inverter and/or the electric motor [9]. The boost converter circuit is shown in Fig. 4.

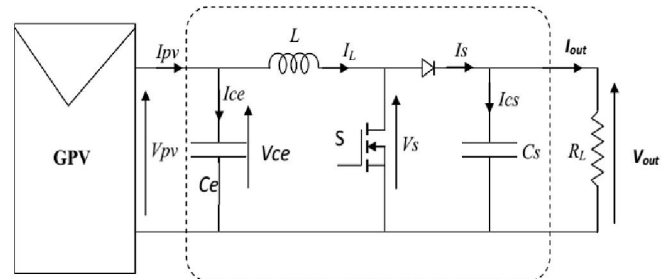


Fig. 4. The DC/DC boost converter

According to the above circuit, as the boost converter is assumed to be ideal, the output voltage and current are related to the photovoltaic ones by the following equations:

$$V_{out} = V_{pv} \frac{1}{1-\alpha} \quad (5)$$

$$I_{out} = I_{pv}(1-\alpha) \quad (6)$$

### C. Inverter modeling

Three-phase voltage source inverters are generally used for induction-motor drives. There exist eight switching states. The voltage vector of the inverter feeding the induction motor is expressed as:

$$V_s = \sqrt{\frac{2}{3}} \cdot [S_a + S_b e^{j\frac{2\pi}{3}} + S_c e^{j\frac{4\pi}{3}}] \quad (7)$$

Where  $S_a$ ,  $S_b$  and  $S_c$  are the inverter switching functions, which takes a logical value (1 or 0).

The stator voltage vectors associated with to the eight sequences of the voltage inverter can be drawn as in Fig. 5.

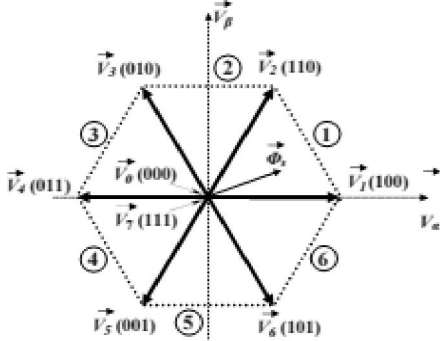


Fig. 5. Switching-voltage space vectors.

#### D. Induction machine modeling

The dynamic behavior of an induction machine is described in terms of space vectors variables as follows [10]:

$$\begin{cases} V_{as} = r_s i_{as} + \frac{d}{dt} \varphi_{as} \\ V_{s\beta} = r_s i_{\beta s} + \frac{d}{dt} \varphi_{\beta s} \\ 0 = r_r i_{\alpha r} + \frac{d}{dt} \varphi_{\alpha r} + \omega_m \varphi_{\beta r} \\ 0 = r_r i_{\beta r} + \frac{d}{dt} \varphi_{\beta r} - \omega_m \varphi_{\alpha r} \end{cases} \quad (8)$$

$$\begin{cases} \varphi_{as} = L_s i_{as} + M i_{\alpha r} \\ \varphi_{\beta s} = L_s i_{\beta s} + M i_{\beta r} \\ \varphi_{\alpha r} = M i_{as} + L_r i_{\alpha r} \\ \varphi_{\beta r} = M i_{\beta s} + L_r i_{\beta r} \end{cases} \quad (9)$$

Where:  $\alpha$  and  $\beta$  indices parameters are the Concordia transformation components of the current and the flux,  $I_{as}, I_{\beta s}$ ,  $I_{\alpha r}$  and  $I_{\beta r}$  are  $\alpha, \beta$  stator and rotor current respectively.  $\varphi_{as}$ ,  $\varphi_{\beta s}$ ,  $\varphi_{\alpha r}$  and  $\varphi_{\beta r}$  are  $\alpha, \beta$  stator and rotor flux respectively,  $R_s, R_r$  are the stator and rotor resistance.  $L_s, L_r, M$  are stator, rotor and magnetizing inductance respectively.

Electromagnetic torque can be expressed in terms of stator current and flux as:

$$T_{em} = \frac{3}{2} P (\varphi_{as} i_{\beta s} - \varphi_{\beta s} i_{as}) \quad (10)$$

Where;  $P$  is the pole pair.

#### E. Centrifugal pump modeling

The flow-head characteristic of a centrifugal pump can be approximated by quadratic form using Pfleider–Peterman model, in which the rotor speed  $\omega$  is a parameter [11]:

$$H = a_0 \omega^2 + a_1 \omega Q + a_2 Q^2 \quad (11)$$

The pump performance is predicted by specifying a load curve. The Q–H characteristic of the pipe network can be expressed by [12]:

$$H = H_g + \psi Q^2 \quad (12)$$

Where,  $H_g$  is the geometrical height which is the difference between the free level of the water to pump and the highest point of the canalization,  $\psi$  is a constant which depends on conduit diameter and on all frictional losses of the pipe network.

The centrifugal pump load torque  $T_r$  is assumed to be proportional to the square of the rotor speed [11]:

$$T_r = C_1 \omega^2 \quad (13)$$

#### IV. MAXIMUM POWER POINT TRACKER (MPPT)

The photovoltaic power characteristics is nonlinear, which vary with the level of solar irradiation and temperature, which make the extraction of maximum power a complex task, considering load variations [13]. As a result, most commercial PV pumping systems either utilize inefficient MPPT control or do not utilize MPPT control at all. Directly connected systems for example operate at the intersection of current–voltage curves of the PV array and the motor-pump set. This operating point may be far from the MPP of the generator wasting a significant proportion of the available solar power. A simple dc–dc converter controlled by an MPPT algorithm can be used as a pump controller to match the PV generator to the motor-pump set [15]. Several methods for extracting the maximum power have been proposed in literature [14].

##### A. Perturb and Observe (P&O)

The P&O MPPT algorithm is mostly used, due to its ease of implementation. It is based on the following criterion: if the operating voltage of the PV array is perturbed in a given direction and if the power drawn from the PV array increases, this means that the operating point has moved toward the MPP and, therefore, the operating voltage must be further perturbed in the same direction. Otherwise, if the power drawn from the PV array decreases, the operating point has moved away from the MPP and, therefore, the direction of the operating voltage perturbation must be reversed [16].

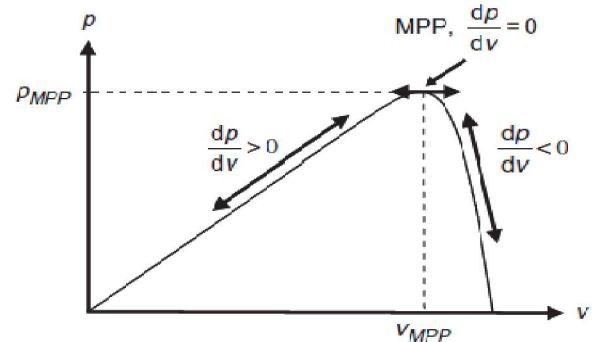


Fig. 6. Power–voltage characteristic of PV panel

Theoretically, the algorithm is simple to implement in its basic form. However, it was noticed some oscillations around the MPP in steady state operating and this causes power loss [17]. Its functioning depends on the tracking step size applied to the voltage reference  $V^*$ . For the same sample time of the system, the oscillations, and consequently the power loss, could be minimized if the tracking step is continuously get smaller [18]. Nevertheless, the response of the algorithm becomes slower. The flow chart of the P&O algorithm is presented in Fig. 6 [19].

### B. Sliding mode control (SMC)

In typical *dc-dc* converter applications, it is desirable to regulate the output voltage to a constant value and the switching surface is chosen according [20]. The SMC such a non-linear control technique represents an effective control method which provides extreme robustness and fast response not only in applications involving switching converters but also for more complex power electronic systems. It is based on the implementation of a control equation which forces the system's variables to stay on a selected surface called "sliding surface". Although a lot of research publications are available in the literature on the SMC, those ones focused in photovoltaic applications are few and mainly devoted on the control of the DC/AC stage for regulating the current injected into the grid, or devoted to perform the Maximum Power Point Tracking (MPPT) as alternative to other MPPT techniques like the Perturb and Observe(P&O) and the Incremental Conductance (INC) [21].

Consider a non-linear system of the form [22]:

$$\dot{x} = f(x, t) + g(x) \cdot u(t) + \Delta d \quad (14)$$

The main steps for sliding mode controller design can be summarized, by using an equivalent control concept, as follows [23]:

- The first step is the selection of a switching surface  $\sigma(x, t) = 0$  (where  $x$  is the system's state vector) that provides the desired asymptotic behavior in steady state.
- Obtaining the equivalent control  $u_{eq}$  by applying the invariance condition

$$\sigma(x, t) = 0 \text{ and } \dot{\sigma}(x, t) = 0 \Rightarrow u(t) = u_{eq} \quad (15)$$

The existence of the equivalent control  $u_{eq}$  assures the feasibility of a sliding motion over the switching surface  $\sigma(x, t) = 0$ . On the other hand, beside describing the average dynamical behavior of the power stage over the switching surface, the equivalent control enables one to obtain the sliding domain, given by:

$$\min \{u^-, u^+\} < u_{eq} < \max \{u^-, u^+\} \quad (16)$$

Where:  $u^-$  and  $u^+$  are the control values for  $\sigma(x, t) < 0$  and  $\sigma(x, t) > 0$ , respectively. The sliding domain is the state plane region where sliding motion is ensured.

- Finally, selecting a non-linear control input  $u_n$  to ensure that Lyapunov stability criteria, i.e.,  $\sigma \dot{\sigma} < 0$ .

### V. DIRECT TORQUE CONTROL (DTC) STRATEGY

In DTC strategies, it is needful to adjust the stator flux, not only is it simple to estimate, but it has a faster dynamic than the rotor flux. The stator flux is given by the Equation (18), which derived from Equation (17) [24].

$$V_s = R_s I_s + \frac{d\varphi_s}{dt} \quad (17)$$

$$\varphi_s(t) = \int_0^t (V_s - R_s I_s) dt \quad (18)$$

The torque and flux are controlled independently by selecting the optimum voltage space vector for entire switching period and the errors are maintained within the hysteresis band [25].

The stator flux amplitude and phase are expressed using Concordia quantities, as follows [24]:

$$\begin{cases} |\varphi_s| = \sqrt{\varphi_{\alpha s}^2 + \varphi_{\beta s}^2} \\ \theta_s = \arctan\left(\frac{\varphi_{\beta s}}{\varphi_{\alpha s}}\right) \end{cases} \quad (19)$$

Table.1. shows the associated inverter switching states of the direct torque control strategy.

TABLE 2

SWITCHING TABLE FOR THE D.T.C STRATEGY

	N	1	2	3	4	5	6
$d_\phi = 1$	$d_\Gamma = 1$	110	010	011	001	101	100
	$d_\Gamma = 0$	111	000	111	000	111	000
	$d_\Gamma = -1$	101	100	110	010	011	001
$d_\phi = 0$	$d_\Gamma = 1$	010	011	001	101	100	110
	$d_\Gamma = 0$	000	111	000	111	000	111
	$d_\Gamma = -1$	001	101	100	110	010	011

### VI. SIMULATION RESULTS

We make simulation of the proposed system (Fig:1.) under Matlab/Simulink for the two MPPT algorithms (P&O, SMC) with the D.T.C which is the suitable control strategy implemented in the induction motor drive. Following a comparative study and obtained simulation results under irradiance 850 w/m<sup>2</sup> and temperature of 27°C are represented.

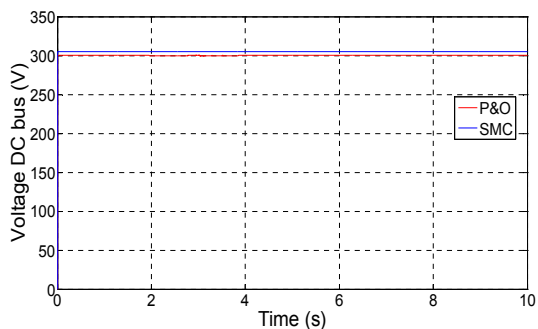


Fig. 7.a. DC bus voltage

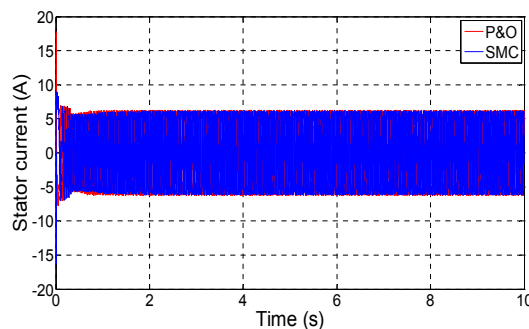


Fig. 7.e. Stator current

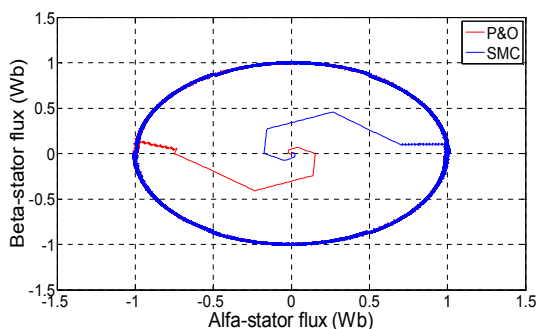


Fig. 7.b. Stator flux trajectory

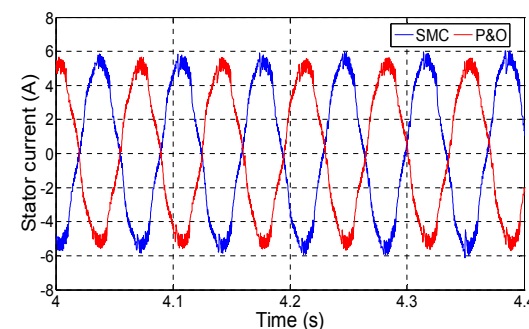


Fig. 7.f. Stator current zoom

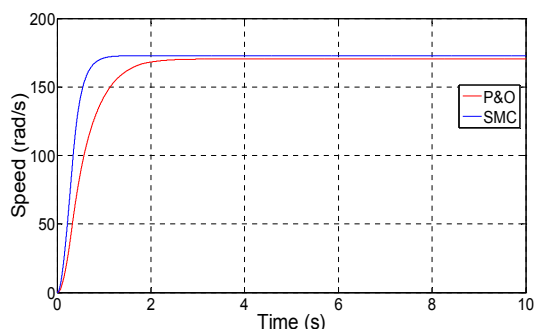


Fig. 7.c. Speed

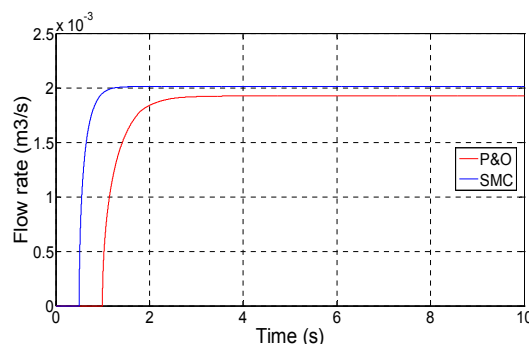


Fig. 7.g. Flow rate

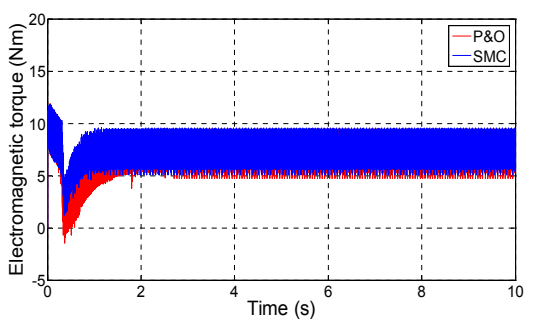


Fig. 7.d. Electromagnetic torque

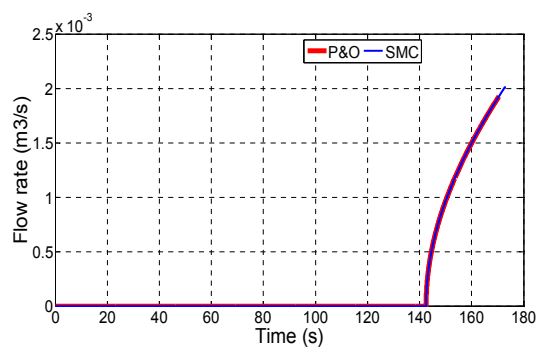


Fig. 7.h. Water flow versus speed

Fig. 7. Simulation results

We note that the voltage DC bus remains constant in both cases with a marked improvement in the sliding mode control. Further investigation of the stator flux has been achieved through the representation of the stator flux vector extremity locus in the  $(\alpha, \beta)$  plane. The obtained results are shown in figure 7.b. One can clearly notice that the two methods yield the smoothest circular locus and keep its reference (1wb). The electromagnetic torque presents a transient increase in oscillatory, then it drops almost instantaneously at a constant value in steady state. Also, with the Sliding mode MPPT method, the speed increases relative to the P&O, resulting in an increase of the water flow.

## VII. CONCLUSION

The main objective of this work is the comparison for the same given set of conditions of two MPPT algorithms, P&O and Sliding Mode Control implemented into the PV pumping system. A Direct Torque Control of an Induction motor fed by a photovoltaic system was proposed in this paper. This allows the extendibility of the applicability of the studied system, particularly in the pumping of water. It is interesting to point out that the differences in performances among the analyzed MPPT are very attractive, and these algorithms must be evaluated according to each use. Nevertheless, this paper contributes for choosing which algorithm should be implemented in the PV power systems. Through this paper, we can conclude that the sliding mode control has good static and dynamic performance (stability and accuracy), that is to say a tolerable response time without overshoot. In addition, it also gives better tracking and allows us to improve the performance of the proposed system with a very high intake of water flow.

## REFERENCES

- [1] M. Aureliano G. De Brito, L. Galotto, Jr., L. P. Sampaio, G. De Azevedo E Melo, And C. A. Canesin "Evaluation Of The Main MPPT Techniques For Photovoltaic Applications" IEEE Transactions On Industrial Electronics, Vol. 60, No. 3, Pp. 1156-1167, March 2013.
- [2] A. Mohammadi, D. Rekioua, N. Mezzi "Experimental Study Of A PV Water Pumping System" *J. Electrical Systems* 9-2 (2013): 212-222.
- [3] B. Subudhi, And R. Pradhan "A Comparative Study On Maximum Power Point Tracking Techniques For Photovoltaic Power Systems" IEEE Transactions On Sustainable Energy, Vol. 4, No. 1, Pp. 89-98, January 2013.
- [4] I. Houssamo, F. Locment, M. Sechilariu "Experimental Analysis Of Impact Of MPPT Methods On Energy Efficiency For Photovoltaic Power Systems" *Electrical Power And Energy Systems* 46 (2013) 98-107
- [5] D. Rekioua, A.Y. Achour, T. Rekioua "Tracking Power Photovoltaic System With Sliding Mode Control Strategy" *Energy Procedia* 36 (2013) 219 - 230.
- [6] T. Noguchi And I. Takahashi "A New Quick-Response And High-Efficiency Control Strategy Of An Induction Motor," *IEEE Trans. Ind. Appl.*, Vol. IA-22, No. 5, Pp. 820-827, Sep./Oct. 1986.
- [7] M. Depenbrock "Direct Self-Control (DSC) Of Inverter-Fed Induction Machine," *IEEE Trans. Power Electron.*, Vol. PE-3, No. 4, Pp. 420-429, Oct. 1988.
- [8] A. Hamidat, B. Benyoucef "Mathematic Models Of Photovoltaic Motor-Pump Systems" *Renewable Energy* 33 (2008) 933-942.
- [9] K. Benlarbi, L. Mokrani, M.S. Nait-Said "A Fuzzy Global Efficiency Optimization Of A Photovoltaic Water Pumping System" *Solar Energy* 77 (2004) 203-216.
- [10] B. Bouzidi, A. Yangui And F. Ben Salem "The Classical And Analytic DTC For Photovoltaic Panel Position And Control" *IJ-STA, Special Issue, CEM, December 2008*, Pp. 636-651.
- [11] A. Betka, A. Attali "Optimization Of A Photovoltaic Pumping System Based On The Optimal Control Theory" *Solar Energy* 84 (2010) 1273-1283.
- [12] A. Betka, A. Moussi "Performance Optimization Of A Photovoltaic, Induction Motor Pumping System" *Renewable Energy* 29 (2004) 2167-2181.
- [13] D. MAG, L.P. Sampaio, L.G. Junior, C.A. Canesin "Evaluation Of MPPT Techniques For Photovoltaic Applications" In: *Proceedings Of The Industrial Electronics (ISIE) 2011 IEEE International Symposium*; 2011. Pp. 1039-44.
- [14] M. A. Eltawila, Z. Zhao "MPPT Techniques For Photovoltaic Applications" *Renewable And Sustainable Energy Reviews* 25 (2013) 793-813.
- [15] M. A. Elgendy, B. Zahawi And D. J. Atkinson "Assessment Of Perturb And Observe MPPT Algorithm Implementation Techniques For PV Pumping Applications" *IEEE TRANSACTIONS ON SUSTAINABLE ENERGY*, VOL. 3, NO. 1 Pp. 21-33, JANUARY 2012.
- [16] N. Femia, G. Petrone, G. Spagnuolo, And M. Vitelli "Optimization Of Perturb And Observe Maximum Power Point Tracking Method" *IEEE TRANSACTIONS ON POWER ELECTRONICS*, VOL. 20, NO. 4, Pp. 963-973, JULY 2005.
- [17] T. Tafticht, K. Agbossou, M.L. Doumbia, A. Chériti "An Improved Maximum Power Point Tracking Method For Photovoltaic Systems" *Renew Energy* 2008; 33(7):1508-16.
- [18] F. Locment, M. Sechilariu, I. Houssamo "Energy Efficiency Experimental Tests Comparison Of P&O Algorithm For PV Power System". In: *Proceedings Of International Power Electronics And Motion Control Conference*; 2010.
- [19] I. Houssamo, F. Locment, M. Sechilariu "Maximum Power Tracking For Photovoltaic Power System: Development And Experimental Comparison Of Two Algorithms" *Renewable Energy* 35 (2010) 2381e2387.
- [20] Y. Levron, D. Shmilovitz "Maximum Power Point Tracking Employing Sliding Mode Control" *IEEE Transactions On Circuits And Systems—I: Regular Papers*, Vol. 60, No. 3, Pp. 724-732, March 2013.
- [21] E. Bianconi, J. Calvente, R. Giral, E. Marnari, G. Petrone, C. Andrés Ramos-Paja, G. Spagnuolo, M. Vitelli "Perturb And Observe MPPT Algorithm With A Current Controller Based On The Sliding Mode" *Electrical Power And Energy Systems* 44 (2013) 346-356.
- [22] I. Kim "Sliding Mode Controller For The Single-Phase Grid-Connected Photovoltaic System" *Applied Energy* 83 (2006) 1101-1115.
- [23] D. Biel, F. Enric "Application Of Sliding-Mode Control To The Design Of A Buck-Based Sinusoidal Generator". *IEEE Trans Industrial Electronics* 2001; 48(3):P563-71.
- [24] B. Metidji, N. Taib, L. Baghli, And T. Rekioua, "Low-Cost Direct Torque Control Algorithm For Induction Motor Without AC Phase Current Sensors," *IEEE Transactions On Power Electronic*, Vol. 27, Pp. 4132-4139, September 2012.
- [25] E. Ozkop, H. I. Okumus "Direct Torque Control Of Induction Motor Using Space Vector Modulation (SVM-DTC)," *Power System Conference*, 12th International Middle-East, Pp. 368-372, March 2008.
- [26] D. Rekioua, E. Matagne, *Optimization Of Photovoltaic Power Systems: Modelization, Simulation And Control*, Edition Springer, 2012.